Room temperature multiferroic effects in superlattice nanocapacitors

S. Dussan, A. Kumar, J. F. Scott, S. Priya, and R. S. Katiyar

Citation: Applied Physics Letters **97**, 252902 (2010); doi: 10.1063/1.3528210
View online: http://dx.doi.org/10.1063/1.3528210
View Table of Contents: http://scitation.aip.org/content/aip/journal/apl/97/25?ver=pdfcov
Published by the AIP Publishing

Room temperature multiferroic effects in superlattice nanocapacitors

S. Dussan,[1] A. Kumar,[1,a)] J. F. Scott,[1,2] S. Priya,[3] and R. S. Katiyar[1,a)]
[1]*Department of Physics and Institute for Functional Nanomaterials, University of Puerto Rico, San Juan, Puerto Rico 00931-3343, USA*
[2]*Department of Physics, Cavendish Laboratory, Cambridge University, Cambridge CB3 0HE, United Kingdom*
[3]*Center for Intelligent Material Systems and Structures (CIMSS), Virginia Tech, Blacksburg, Virginia 24061, USA*

(Received 8 September 2010; accepted 24 November 2010; published online 21 December 2010)

A composite nanocapacitor was fabricated based on ferroelectric $PbZr_{0.52}Ti_{0.48}O_3$(PZT) and half-metallic oxide $La_{0.67}Sr_{0.33}MnO_3$(LSMO) with 5 nm/1 nm periodicity, respectively. X-ray θ-2θ scan and Φ-scan revealed epitaxial growth of nanocapacitors. At room temperature, a microscopic polarization of 11 $\mu C/cm^2$ and magnetization of 50 emu/cm^3 were measured for superlattice nanocapacitors. Local piezo force microscopy measurements revealed switching of polarization under external bias field confirming ferroelectric behavior. Zero field cooling measurements showed the existence of cusp in magnetization at low temperatures indicating spin-glass-like behavior contrary to $Pb(Zr_xTi_{1-x})O_3/La_xSr_{1-x}MnO_3$ bilayer structure. Frequency dependent dielectric anomaly was observed near room temperature suggesting dynamic magneto (resistance)-dielectric coupling. © *2010 American Institute of Physics*. [doi:10.1063/1.3528210]

Multiferroic magnetoelectrics (ME) are attractive class of multifunctional materials exhibiting coupling between two or more ferroic orders [e.g., ferroelectric (FE), ferromagnetic (FM), and/or ferroelastic]. This ferroic coupling makes these materials attractive candidates for potential applications in memories devices and magnetic field sensors.[1–7] However, there are limited numbers of naturally existing single-phase multiferroic magnetoelectrics which is expected based on the fact that ferromagnetism and ferroelectricity are often incompatible as one requires empty d-orbitals while the other expects them to be partially filled. These problems have been overcome by synthesizing composites based on product rule utilizing elastic coupling. Several approaches have been adopted to synthesize artificial structures that exhibit magnetoelectric coupling.[7] One of these possibilities is FE and FM layered structures or laminates with 2–2 connectivity which has been widely explored in literature. However, the main problem of this architecture in applications for memories is its delayed switching due to strain-dependent coupling occurring at the interface.[8] The response is dependent on magnetoelastic and elastoelectric coupling which is mainly governed by the mechanical impedance mismatch across the interface. The other structures are superlattices composed of FE and FM thin layers, which yield large magnetoelectric effect via strong electromagnetostrictions due to reduced role of interfaces.[9–12]

Ferroelectric lead zirconate titanate $Pb(Zr_xTi_{1-x})O_3$ (PZT) is common constituent of the superlattice structures owing to its high Curie temperature (T_C), low coercive field (E_c), and high remanent polarization (P_r). These properties also make PZT an excellent candidate for nonvolatile random access memories.[8,13] To complete the superlattice structure, $La_xSr_{1-x}MnO_3$ (LSMO) is a good candidate, both as ferromagnetic-layer in the sandwich and as the bottom electrode. LSMO is known to exhibit high Curie temperature of about 370 K, colossal magnetoresistance[14] properties, and half-metallic behavior.[15] Further, its lattice parameter (3.87 Å) matches closely to that of perovskite ferroelectric material. Our previous work[16] has demonstrated dynamic magnetodielectric interaction in bilayered PZT/LSMO thin films that was attributed to Parish–Littlewood mechanism of inhomogeneity near the metal-dielectric interface. In addition, multiferroic properties have been reported in epitaxial $La_{0.7}Sr_{0.3}MnO_3/PbZr_xTi_{1-x}O_3$ heterostructures which makes this system worthy of further investigation.[17]

In this study, we focus on fabrication of series architecture of nanocapacitors as shown in inset of Fig. 1 and investigate their electrical, dielectric, magnetic, magnetodielectric, negative magnetization in zero field cooled (ZFC) and spin-glass like properties as function of temperature and frequency.

Superlattices (SLs) with a periodicity of 5nm/1 nm of $PbZr_{1-x}Ti_xO_3$ (x=0.48) (PZT)/$La_{1-x}Sr_xMnO_3$ (x=0.33) (LSMO) were fabricated by using pulsed laser deposition (PLD) with total thickness of around 360 ± 10 nm. The detailed deposition parameters and electrical characterization are discussed elsewhere.[16] Scanning probe microscopy (Veeco-AFM contact mode) was used to examine the surface topography, piezo force microscopy (PFM) surface roughness, and local ferroelectric switching behavior. Magnetic hysteresis, Zero-field cooled (ZFC) and field cooled (FC) magnetization were measured by using a Quantum Design MPMS XL-7 superconducting quantum interference device magnetometer (SQUID).

Figure 1(a) shows the θ-2θ x-ray scan around the (200) fundamental peak (38°–52° in 2θ) of $(PZT_{12\ u.c}/LSMO_{3\ u.c})_{60}$ superlattice. The number $n = \pm 1$ indicates the nth satellite peak, clearly demonstrating that the periodically modulated structure was achieved. The modulation period was $\Lambda = 6$ nm calculated from relation $\Lambda = \lambda/(2 \times (\sin\theta_{n+1} - \sin\theta_n))$, where λ is the x-ray wavelength and θ_{n+1}, θ_n are the angular position of two adjacent SL satellite peaks.[18] In order to examine the in-plane crystallographic coherence, a Φ-scan shown in Fig. 1(b) was realized around (202) plane with the axis normal to the plane of substrate. Four peaks at

a)Authors to whom correspondence should be addressed. Electronic addresses: ashok553@gmail.com and rkatiyar@uprrp.edu.

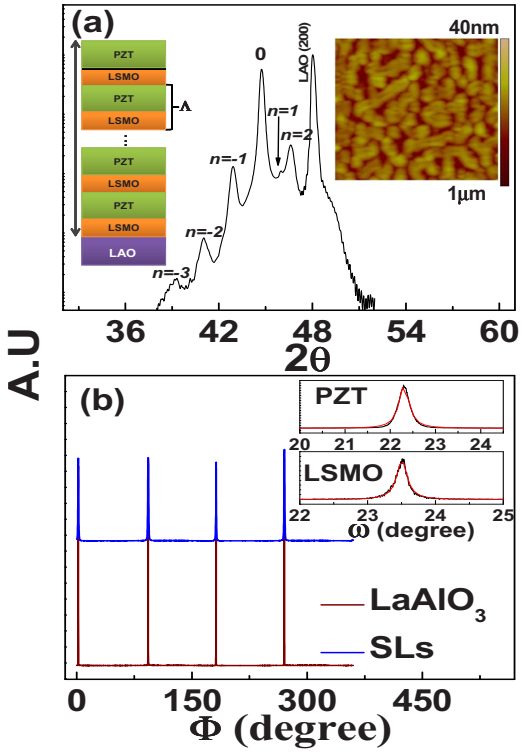

FIG. 1. (Color online) θ-2θ XRD pattern of (PZT)/(LSMO) superlattices (SLs) on LAO substrate, topography of 1 μm×1 μm×40 nm z-scale (inset). The inset shows Φ-scan around (202) and (220) reflections of the SL and substrate, respectively. Rocking curve is shown in the inset. Rocking curve is shown in the inset, with FWHM 0.27° and 0.19° for PZT and LSMO, respectively.

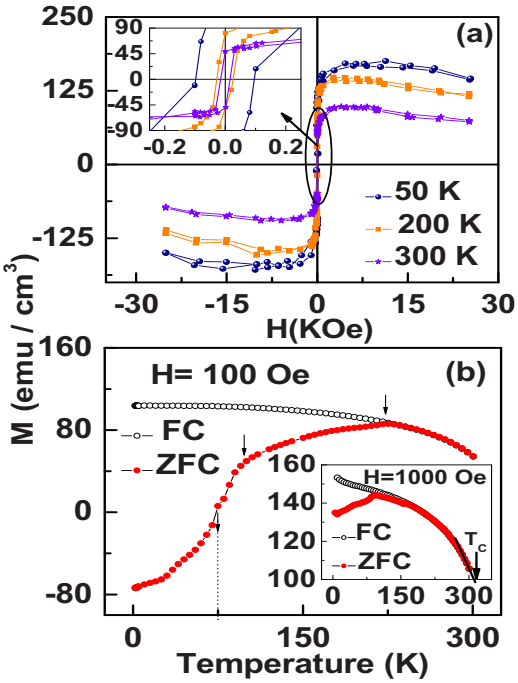

FIG. 2. (Color online) Field dependence of magnetic hysteresis curves at different temperatures (a) and temperature dependent ZFC and FC magnetization (m) measured in 100 Oe applied magnetic field (b) of PZT/LSMO SLs.

the interval of 90° spacing from each other were clearly observed, indicating the fourfold symmetry. The Φ-scan shows the same rotation angles as those of the LAO (220) which confirms that the SLs were grown epitaxially block-by-block. The in-plane lattice parameters of oriented PZT and LSMO grown on LAO (001) were found to be $a(\text{Å})_{PZT}=4.0472$ and $a(\text{Å})_{LSMO}=3.9139$ which is slightly higher as compared to bulk counterpart $a'(\text{Å})_{PZT}=4.0362$ and $a'(\text{Å})_{LSMO}=3.8715$. These data indicate that the epitaxial films were relaxed. The central peak ($a(\text{Å})=4.0622$) of superlattice showed small (~0.64%) in-plane tensile strain compared to bulk $a'(\text{Å})_{PZT}=4.0362$ calculated using the equation $\varepsilon=a_{PZT(bulk)}-a_{SL}/a_{PZT(bulk)}\times 100$. The full width at half maximum of the rocking curve of 202 peak of PZT and LSMO were found to be 0.27° and 0.19°, suggesting high crystalline quality [inset of Fig. 1(b)]. Surface topography showed homogeneous surface of the films with average roughness of 1.5 nm [inset Fig. 1(a)].

Ferromagnetic behavior of SL due to LSMO layers was demonstrated from the magnetic hysteresis loops measured at 50, 200, and 300 K as shown in Fig. 2(a). The coercive fields were 97, 27, and 16 Oe, respectively [inset Fig. 2(a)] under application of 25 KOe external magnetic field. The temperature dependent ZFC and FC magnetization curves are shown in Fig. 2(b). These measurements show splitting around 230 K (under 100 Oe) indicating thermomagnetic irreversibility ($M_{ZFC}\neq M_{FC}$) and the irreversibility effect, M_{irr} ($M_{FC}-M_{ZFC}$) which decreases in the presence of strong magnetic field (1000 Oe). This type of irreversibility in magnetization (thermomagnetic hysteresis) and the cusps that appear in ZFC curves are typically characteristic of cluster-spin glass systems.[19–22] In our system, this phenomenon may be attributed to the disordered distribution of Mn^{3+} and Mn^{4+} ions and the competition between FM and antiferromagnetic (AFM) interactions.[20] Further, spin-glass behavior may be ascribed to the diffusion of domain walls. The negative magnetization observed in ZFC curve (100 Oe) below 75 K could be interpreted as (i) an artifact due to small negative field trapped in the superconducting magnet[21] or (ii) as an AFM coupling between uncompensated spins trapped across ferroelectric-ferromagnetic interface and ferroelectric domain wall. We believe that the latter interpretation is more applicable in our case based on the PFM measurements that indicated pinning of domain boundary. Negative magnetization in ZFC curves has been observed in polycrystalline $CoCr_2O_4$, which was attributed to the trapped spins across the grain boundary.[22] This effect only persists at low magnitude of ZFC external magnetic field (<100 Oe). The experimental Curie temperature (T_C~312 K) was determined by linear extrapolation of the magnetization to the base line in ZFC/FC measurements at applied magnetic field of 1000 Oe. This value is slightly smaller than that reported magnitude for bulk $La_{0.67}Sr_{0.33}MnO_3$, whose T_c was found to be around 350 K. The reduction of ferromagnetism in SL was associated with the effect of in-plane tensile strain experienced by the ultrathin (~1 nm) LSMO (a=3.871 Å) layers sandwiched between 5 nm PZT (a=4.036 Å) layers.

The variation of ferromagnetic T_C as a function of strain can be expressed[23] as $T_C(\epsilon)=T_C(\epsilon=0)(1-\alpha\epsilon_B-1/2\Delta\epsilon'^2)$, where ϵ_B is bulk strain, ϵ' is Jahn–Teller (JT) strain and α and Δ represent the relative weight of symmetry-conserving bulk strain and symmetry-breaking JT strain, respectively. Therefore, the decrease in T_C is larger for $\epsilon_B>0$ (tensile strain) than $\epsilon_B<0$ (compressive strain). Figure 3(a) shows the room temperature electric field dependence of dielectric constant at different frequencies for PZT/LSMO SL. The SL

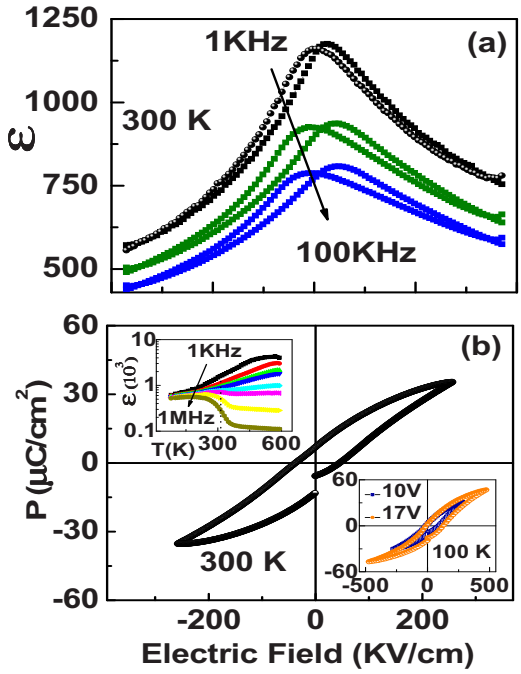

FIG. 3. (Color online) (a) Room temperature electric field dependence of dielectric constant for different frequencies; (inset) temperature dependent dielectric constant at different frequencies. (b) (P-E) hysteresis loops at room temperature; (inset at 100 K).

structure exhibited a typical butterfly curve expected for a ferroelectric material. The dielectric tunability of 35% was calculated from relation $|\varepsilon_{(0)}-\varepsilon_{(E)}|/\varepsilon_{(0)}$, where $\varepsilon_{(0)}$ and $\varepsilon_{(E)}$ are the dielectric constant at zero and applied electric field E, respectively. The ferroelectric hysteresis loop (P-E) at 300 K and 1 kHz frequency under a maximum applied electric field of 250 kV/cm is shown in Fig. 3(b). The measured remnant polarization was found to be $P_r=11\ \mu C/cm^2$ with coercive field of 42 kV/cm. The low temperature P-E measurements at different applied voltages and 50 Hz frequency are shown in inset of Fig. 3(b).

The effect of ferromagnetic transition of LSMO on the dielectric constant (ε) in the SL structure is shown in the inset of Fig. 3(b). The measurements were conducted in the temperature range of 100–600 K and frequency range of 10^2–10^6 Hz. It can be seen that dielectric constant exhibits strong frequency dispersion with a rapid decrease in the magnitude at higher frequencies close to the semimetal ferromagnetic to semi-insulating paramagnetic phase transitions. These results are in accordance with the Cole-Cole plot (not shown here) which indicated shifting of relaxation frequency to lower side with increase in temperature. The potential cause of this behavior is related to the metal-ferromagnetic to insulator-paramagnetic (M-I) transition of LSMO which exhibits conductor behavior at low frequency in the vicinity of M-I transition, whereas it becomes insulating at high frequencies $>10^4$ Hz. We observe a dielectric anomaly below 314 K where the FM ordering emerges. This sharp increase in dielectric constant is signature of dynamic coupling among the dielectric, magnetic, and electric properties of LSMO.

Switching behavior of ferroelectric domains was investigated by using scanning probe microscopy and lock-in amplifier technique. We applied dc bias voltage between the LSMO bottom electrode and conducting AFM tip. Positive and negative bias voltages (+/−8 V) greater than the coercive field were employed to switch the domains which in turn results in opposite contrast in phase and amplitude image as can be seen in Fig. 4. These observations suggest that we can switch polarization of 5 nm capacitor with 1 nm magnetic electrode locally as well as globally (Fig. 3).

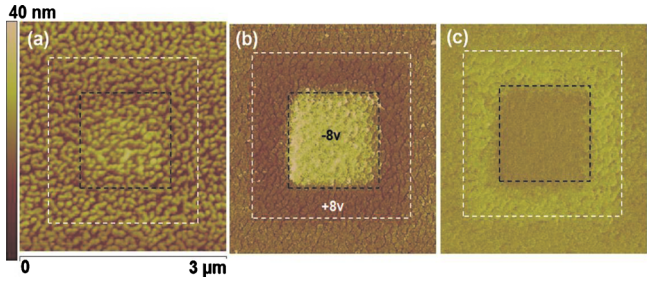

FIG. 4. (Color online) PFM image of 3 μm×3 μm×40 nm z-scale of SLs (i) topography after poling, (ii) phase image of −/+8 V poling, (iii) amplitude image of −/+8 V poling.

In summary, we have epitaxially grown 5 nm PZT capacitors connected in series with 1 nm conducting LSMO electrode. We directly measured large polarization for 100 μm^2 electrode area and switching of local polarization by PFM for these nanocapacitors. Series connected nanocapacitors exhibited room temperature multiferroics properties. Low magnetic field ZFC data indicated spin-glass-like behavior in SL unlike to that of bilayer structure. Dynamic magnetoresistive-dielectric coupling was observed in the vicinity of magnetic phase transition.

This work was partially supported by DoE FG 02-08ER46526 and NSF-RII-0701-525 grants to UPR.

[1]N. A. Spaldin and M. Fiebig, Science **309**, 391 (2005).
[2]Ce-Wen Nan M. I. Bichurin, S. Dongb, D. Viehland, and G. Srinivasan, J. Appl. Phys. **103**, 031101 (2008).
[3]A. Barthélémy and M. Bibes, Nature Mater. **7**, 425 (2008).
[4]W. Eerenstein, M. Wiora, J. L. Prieto, J. F. Scott, and N. D. Mathur, Nature Mater. **6**, 348 (2007).
[5]N. A. Hill, J. Phys. Chem. B **104**, 6694 (2000).
[6]C. Ederer and N. A. Spaldin, Nature Mater. **3**, 849 (2004).
[7]R. Ramesh and N. A. Spaldin, Nature Mater. **6**, 21 (2007).
[8]J. F. Scott and C. A. Paz de Araujo, Science **246**, 1400 (1989).
[9]M. P. Singh, W. Prellier, L. Mechin, Ch. Simon, and B. Raveau, J. Appl. Phys. **99**, 024105 (2006).
[10]P. Murugavel, P. Padhan, and W. Prellier, Appl. Phys. Lett. **85**, 4992 (2004).
[11]P. Murugavel, D. Saurel, W. Prellier, Ch. Simon, and B. Raveau, Appl. Phys. Lett. **85**, 4424 (2004).
[12]P. Padhan, P. LeClair, A. Gupta, M. A. Subramanian, and G. Srinivasan, J. Phys.: Condens. Matter **21**, 306004 (2009).
[13]O. Auciello, J. F. Scott, and R. Ramesh, Phys. Today **51**(7), 22 (1998).
[14]A. Urushibara, Y. Moritomo, T. Arima, A. Asamitsu, G. Kido, and Y. Tokura, Phys. Rev. B **51**, 14103 (1995).
[15]J. H. Park, E. Vescoso, H. J. Kim, C. Kwon, R. Ramesh, and T. Venkatesan, Nature (London) **392**, 794 (1998).
[16]S. Dussan, A. Kumar, J. F. Scott, and R. S. Katiyar, Appl. Phys. Lett. **96**, 072904 (2010).
[17]M. Ziese, A. Setzer, I. Vrejoiu, B. I. Birajdar, B. J. Rodriguez, and D. Hesse, J. Appl. Phys. **104**, 063908 (2008).
[18]E. E. Fullerton, I. K. Schuller, H. Vanderstaeten, and Y. Bruynseraede, Phys. Rev. B **45**, 9292 (1992).
[19]A. Kumar, R. S. Katiyar, C. Rinaldi, S. G. Lushnikov, and T. A. Shaplygina, Appl. Phys. Lett. **93**, 232902 (2008).
[20]C. S. Xiong, Y. H. Xiong, W. Yi, G. N. Meng Z. C. Xia, X. G. Li, and S. L. Yuan, J. Phys.: Condens. Matter **14**, 4309 (2002).
[21]N. Kumar and A. Sundaresan, Solid State Commun. **150**, 1162 (2010).
[22]G. Lawes, B. Melot, K. Page, C. Ederer, M. A. Hayward, Th. Proffen, and R. Seshadri, Phys. Rev. B **74**, 024413 (2006).
[23]H. S. Wang, E. Wertz, Y. F. Hu, Q. Li, and D. G. Schlom, J. Appl. Phys. **87**, 7409 (2000).